International Journal of Fracture (2005) 133:61–87
DOI 10.1007/s10704-005-2183-0

A unified treatment of the mode I fatigue limit of components containing notches or defects

B. ATZORI[1,*], P. LAZZARIN[2] and G. MENEGHETTI[1]
[1]*Department of Mechanical Engineering, University of Padova, via Venezia 1, 35131, Padova, Italy*
[2]*Department of Management and Engineering, University of Padova, Stradella S. Nicola 3, 36100 Vicenza, Italy*
[*]*Author for Correspondence (E-mail: bruno.atzori@unipd.it)*

Received 15 November 2004; accepted in revised form 14 February 2005

Abstract. The paper addresses the estimation of the fatigue limit of components weakened either by U- and V-shaped notches or by defects, all under mode I stress distributions. When the influence of the opening angle is absent, a single formula is able to summarise both the notch sensitivity and the sensitivity to defects. Fatigue limit assessments need two material parameters, namely the plain fatigue limit and the threshold value of the long crack stress intensity factor range. The formula is compared with about 90 fatigue limits taken from the literature. Material properties and specimen geometries are given in detail. Afterwards, in the case of V-notches with large opening angles, the formula is modified, but without involving additional material parameters. A generalised Kitagawa diagram is obtained, that encompasses fatigue behaviour of stress raisers of different size, opening angle and notch tip radius.

Key words: Defect sensitivity, fatigue limit, notch sensitivity, stress intensity, V-notch.

List of symbols

a	=	reference dimension of a component, for example the notch depth,
a^*, a^*_γ	=	characteristic values of "a" for a U- and a V-notched component, respectively,
a_D, $a_{D\gamma}$	=	cut-off values of "a" for a U- and a V- notched component, respectively,
ρ	=	notch tip radius,
r, θ	=	polar coordinates,
K_{tg}	=	elastic stress concentration factor referred to the gross section of the specimen,
K_{tg}*	=	characteristic value of K_{tg},
K_f	=	fatigue strength reduction factor,
K_I	=	mode I Stress Intensity Factor,
ΔK_{th}	=	threshold range of mode I Stress Intensity Factor,
K_I^V	=	mode I Notch-Stress Intensity Factor for a sharp V-notch,

$\Delta K^{V}_{I,th}$ = threshold range of mode I Notch-Stress Intensity Factor,
σ_g = gross nominal stress,
$\Delta\sigma_g$ = range of the gross nominal stress,
$\Delta\sigma_{g,th}$ = threshold range of the gross nominal stress,
$\Delta\sigma_0$ = plain specimen fatigue limit (in terms of stress range),
σ_y = yield strength,
R = nominal stress ratio,
a_0 = El Haddad-Smith-Topper material constant used in Fracture Mechanics studies,
a_0^V = characteristic length parameter for a V-notched component,
α = geometric shape factor for a component containing a crack,
α_γ = non-dimensional coefficient, dependent on component geometry, loading type and notch opening angle,
$\alpha_{0\gamma,\bar{w}}$, $\alpha_{0\gamma,LEFM}$, $\alpha_{0\gamma,PM}$ = non-dimensional coefficients derived by means of the local energy, the fracture mechanics and the point method approaches, respectively,
φ = V-notch opening angle,
γ = degree of singularity of the stress distributions.

1. Introduction

The different behaviour of blunt and sharp notches has been known for a long time (Frost et al., 1974; Smith and Miller, 1978). It is generally described in the so-called Frost–Miller diagram shown in Figure 1 where the two curves are drawn by keeping the notch depth "a" constant and varying the notch tip radius. The two curves intersect at a particular value of the stress concentration factor referred to the gross section, named K^*_{tg}. When K_{tg} is lower than K^*_{tg}, the fatigue limit of the notch in terms of nominal stress referred to the gross section is $\Delta\sigma_{g,th} = \Delta\sigma_0/K_{tg}$, $\Delta\sigma_0$ being the material fatigue limit under the same load conditions. In other words the fatigue limit is fully controlled by the range of the elastic peak stress $\Delta\sigma_{peak}$. When K_{tg} is greater than K^*_{tg}, the notch behaves as a crack with the same depth "a" and the fatigue limit can be estimated by means of the Linear Elastic Fracture Mechanics (LEFM) according to the expression $\Delta\sigma_{g,th} = \Delta K_{th}/(\alpha \cdot \sqrt{\pi a})$, where ΔK_{th} is the threshold value of the stress intensity factor range for long cracks under the same load conditions and α is a shape coefficient calculated for a crack having the same depth of the real notch. The characteristic K^*_{tg} value ideally separates the regions of applicability of the two criteria. As well known, beyond the branch point located in correspondence of K^*_{tg}, there exist two different fatigue limits: the lower one is the critical stress for crack nucleation; the higher one is the threshold stress of small cracks initiated at the notch

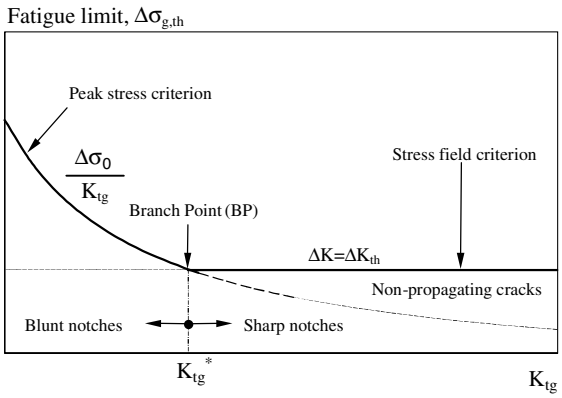

Figure 1. Fatigue limit in terms of nominal stress range $\Delta\sigma_{g,th}$ vs. the theoretical stress concentration factor K_{tg} for notches of constant depth a.

tip but unable to propagate beyond a certain distance from it (Smith and Miller, 1978; Nisitani and Endo, 1988).

Recently, Atzori and Lazzarin proposed for notched components a generalisation of the Kitagawa diagram valid for cracked components (Kitagawa and Takahashi, 1976; Atzori and Lazzarin, 2001). The diagram is valid for a notch with parallel flanks centred in an infinite plate and subjected to a remotely applied tensile stress (Figure 2). It was drawn by analytically evaluating the fatigue limit of the notch with respect to a scale variation of its absolute dimensions, being the stress concentration factor unchanged. Given a certain notch acuity ζ, defined as the ratio between the notch depth a and the root radius ρ (thus the stress concentration factor is fixed), the fatigue limit is simply given by $\Delta\sigma_0/K_{tg}$, if the absolute dimensions are sufficiently high. By reducing the notch dimensions the fatigue behaviour conforms to the ΔK_{th} line when the notch depth a becomes smaller than the characteristic value a^*. Schematically, if the notch depth is between a_0 and a^*, then the fatigue behaviour is fully governed by the LEFM (so that the fatigue limit is equal to that of a crack having the same size), being a_0 the El Haddad-Smith-Topper parameter (El-Haddad et al., 1979), defined as:

$$a_0 = \frac{1}{\pi}\left(\frac{\Delta K_{th}}{\Delta\sigma_0}\right)^2. \tag{1}$$

When $a > a^*$, the notch sensitivity is full; on the other side, when $a < a_0$ the fatigue limit approaches the material fatigue limit.

The two length parameters are correlated to each other by means of the simple expression (Ting and Lawrence, 1993; Atzori and Lazzarin, 2001)

$$a^* = K_{tg}^2 a_0. \tag{2}$$

Dealing with cracks, El-Haddad-Smith-Topper proposed the following expression to estimate the fatigue limit of both long and short cracks (El-Haddad et al., 1979):

$$\Delta K_{th} = \Delta\sigma_{g,th}\sqrt{\pi\,(a+a_0)}. \tag{3}$$

This expression shows a dependency of the type $\Delta\sigma_{g,th}^2 \cdot a = \text{const}$ only for long cracks. In the past, Frost (1961) proposed the relation $\Delta\sigma_{g,th}^3 \cdot a = \text{const}$, where the different value of exponent was due to the particular range of crack lengths that had been measured during experiments, as pointed out by Murakami and Endo (1994).

In the case of real components it is necessary to account for a shape coefficient α (Du Quesnay et al., 1988). A convenient form for Equation (3) is then (Atzori et al., 2003)

$$\Delta K_{th} = \Delta\sigma_{g,th}\sqrt{\pi\left(\alpha^2 a + a_0\right)}. \tag{4}$$

In this expression a_0 continues to be the material parameter obeying Equation (1). It depends on the nominal load ratio R, but not on the geometry of the component. By so doing, the diagram already shown in Figure 2 is still valid, provided that the notch depth a is substituted by $(\alpha^2 a)$. That diagram was validated by the present authors by means of a number of experimental data reported in the literature for different materials, notch geometries and loading conditions (Atzori et al., 2003, 2004).

The diagrams of Figures 1 and 2, showing the notch behaviour from two different viewpoints, were summarised in a single three dimensional diagram where the fatigue limit of a notched components was plotted as a function of both the stress concentration factor K_{tg} and the parameter $(\alpha^2 a)$ (Atzori and Lazzarin, 2002). A slightly modified version of that three-dimensional diagram is shown in Figure 3, where $(\alpha^2 a)$ is substituted by an equivalent length a_{eq}, as discussed later.

It is well known that the fatigue behaviour described by Figures 1 and 2 is schematic, a gradual transition from the peak criterion (controlled by K_{tg}) to the field criterion (controlled by ΔK_{th}) really taking place. Then in Figure 2, there are two transition zones, where the material exhibit a sensitivity to notches (close to a^*) and a sensitivity to defects (close to a_0).

The aim of this paper is to provide an equation for estimating the fatigue limit for different stress raisers (i.e. defects, cracks, crack-like notches and blunt notches with a small opening angle) and to extend the Kitagawa diagram to V-shaped notches having large opening angles and an arbitrary notch root radius.

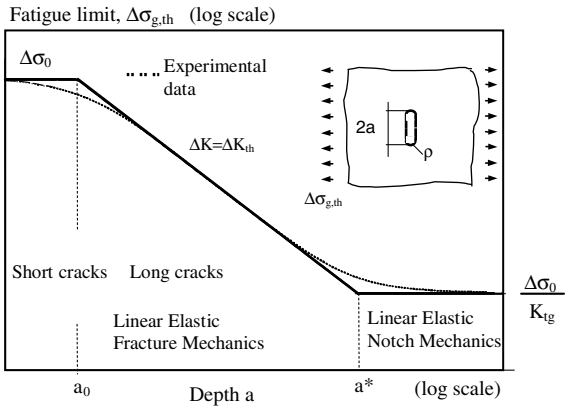

Figure 2. Scale effect in the fatigue behaviour of a crack or a notch.

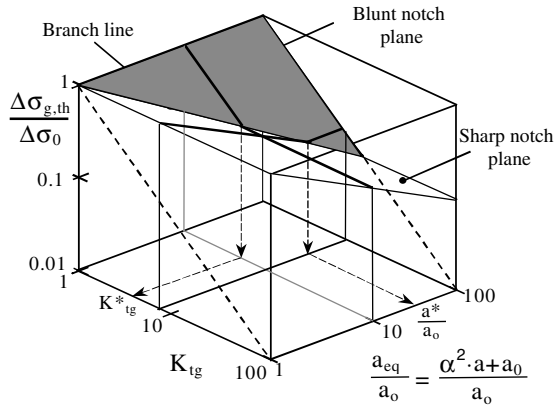

Figure 3. Fatigue limit of notched components in terms of an equivalent notch size equal to $(\alpha^2 \cdot a + a_0)$ (Atzori et al., 2002b).

2. Fatigue strength of U-notches

Equation (4) valid for short and long cracks can be re-written in the following way:

$$\Delta K_{th} = \Delta\sigma_{g,th}\sqrt{\pi a_{eq}}, \tag{5}$$

where

$$a_{eq} = \alpha^2 a + a_0. \tag{6}$$

In Equation (5) the quantity $(\alpha^2 a + a_0)$ can be thought of as the length a_{eq} of an equivalent crack centred in an infinite plate and subjected to the same gross nominal stress applied to the real component. By using the definition for a_0 given by Equation (1), Equation (5) becomes

$$\frac{\Delta\sigma_{g,th}}{\Delta\sigma_0} = \frac{1}{\sqrt{\frac{\alpha^2 a + a_0}{a_0}}} = \sqrt{\frac{a_0}{a_{eq}}}. \tag{7}$$

On the other hand, blunt notches obey the following simple equation:

$$\frac{\Delta\sigma_{g,th}}{\Delta\sigma_0} = \frac{1}{K_{tg}}. \tag{8}$$

By equating the right hand sides of Equations (7) and (8), one can find the characteristic value K^*_{tg} that ideally separates sharp and blunt notch behaviour

$$K^*_{tg} = \sqrt{\frac{\alpha^2 a + a_0}{a_0}}. \tag{9}$$

In Equation (9) the parameter $\alpha^2 a$ quantifies the influence of the absolute dimensions of the component. By combining Equations (2) and (9), one obtains the link between the characteristic parameters K^*_{tg} and a^*

$$\frac{K^*_{tg}}{K_{tg}} = \sqrt{\frac{a_{eq}}{a^*}}. \tag{10}$$

Making use of Equations (7) and (8), the three dimensional diagram can be presented in the form shown in Figure 3, where the equivalent notch depth and the stress concentration factor are used as design variables (Atzori et al., 2002b). By so doing two intersecting planes can be obtained

the sharp notch plane (defined by Equation (7) for a given K_{tg}, value);
the blunt notch plane (defined by Equation (8) for a given equivalent notch size).

The two planes intersect in correspondence of a so-called branch line (Nisitani and Endo, 1988), where fatigue behaviour switches from one regime to the other, according to the present schematic representation. Intersections of the three dimensional diagram with planes which are normal to the K_{tg} axis provide the modified Kitagawa diagram recently proposed by Atzori and Lazzarin for given K_{tg} values. Conversely, intersections with planes normal to the a_{eq}/a_0 axis provide the classical Frost–Miller diagram for a given notch size.

Figure 3 illustrates how to derive a^*, for a given K_{tg} value, and K_{tg}^*, for a given a_{eq} value, while dealing with a notch characterised by an equivalent depth a_{eq} and a stress concentration factor K_{tg}. Practical use of such parameters will be illustrated later on.

Validation of the diagram proposed by Atzori and Lazzarin has already been presented in other papers (Atzori et al., 2002b, 2003). In the present work, in order to put in evidence the experimental behaviour of different materials near to the branch point, the two dimensional diagrams derived by intersecting the three dimensional diagram reported in Figure 3 will be presented in a different, non-dimensional form.

All experimental data were taken from the literature. The considered materials are listed in Table 1 and include low strength steels, carbon steels, high strength steels, wrought aluminium alloys and one cast aluminium alloy. Both static (yield strength σ_y) and fatigue properties ($\Delta\sigma_0$, a_0 and ΔK_{th} for a given load ratio R) have been reported in the table. We note that both $\Delta\sigma_0$ and ΔK_{th} are expressed in terms of range, i.e. maximum minus minimum value. Concerning the R-ratio effects, they are included in the parameter a_0, which is influenced by both the mean stress effect on the fatigue limit and the crack closure effect on ΔK_{th}. In order to avoid the dependence on crack closure, the effective component of the threshold stress intensity factor range should be adopted. Nevertheless the data found in the literature usually do not report the effective component of ΔK_{th} so that the authors adopted the original El Haddad-Smith-Topper parameter a_0, defined by ΔK_{th} and $\Delta\sigma_0$. With respect to a previous synthesis (Atzori et al., 2003), Table 1 summarises additional data obtained by the present authors by testing a low carbon deep drawing steel and a cast aluminium alloy, both used in European automotive manufacturing. Figure 4 together with Tables 2 provides details on the notch and defects geometries, loading conditions, stress concentration factors and shape factors. From Table 2 the wide variation of notch acuities can be appreciated, ranging from 0.1 up to about 100. The re-analysis presented here will include also 26 fatigue limits obtained in the past by Murakami and Endo (1983) by testing specimens containing artificial defects, more precisely the small drilled holes shown in Figure 4. All these data are reported in Table 3. Values of ΔK_{th} of the relevant materials are reported in Table 1, taken from the literature (Akiniwa et al., 1997; McEvily et al., 2003). Then, about 90 experimental fatigue

Table 1. Materials and mechanical properties.

Materials	References	σ_y (MPa)	$\Delta\sigma_0$ (MPa)	a_0 (μm)	ΔK_{th} (MPa·m$^{0.5}$)	R
Annealed 0.45 carbon steel	(Nisitani and Endo, 1988)	364	582	61[a]	8.1[a]	−1
Annealed 0.36 carbon steel	(Nisitani and Endo, 1988)	/	446[a]	92[a]	7.6[a]	−1
Annealed 0.46 carbon steel	(Murakami and Endo, 1983) (Akiniwa et al., 1997)	284	480	152	10.5	−1
Annealed 0.13 carbon steel	(Murakami and Endo, 1983) (McEvily et al., 2003)	206	362	294	11	−1
SAE 1045 steel	(Du Quesnay et al., 1988)	466	606	70	9.0	−1
2024-T351 Al alloy	(Du Quesnay et al., 1988)	360	172	172[b]	4.0	0
2024-T351 Al alloy	(Du Quesnay et al., 1988)	360	248	100[b]	4.4	−1
G40.11 steel	(Du Quesnay et al., 1988)	376	540	144	11.5	−1
Mild steel (0.15% C)	(Frost, 1959) (Harkegard, 1981)	340	420	296	12.8	−1
NiCr steel	(Frost, 1957) (Harkegard, 1981)	834	1000	52	12.8	−1
304 stainless steel	(Ting and Lawrence, 1993) (Harkegard, 1981)	222	720	88	12.0	−1
FeP04 steel	(Lazzarin et al., 1997)	185	247	522	10	0.1
AA 356-T6 cast Al alloy	(Lazzarin et al., 1997)	182	140	406	5	0.1

[a] Values estimated by means of a best fitting of experimental results based on Equation (4).
[b] Determined by means of Equation (1).

limits of specimens containing notches and defects have been considered in the present contribution.

Figure 5 presents the experimental fatigue limits in the diagram obtained by intersecting the three dimensional diagram with planes perpendicular to the K_{tg} axis (Atzori and Lazzarin, 2002). By so doing the size effect found for the sharp notches is described by the sloping line of the diagram. Conversely, the size effect is null for blunt notches, as shown by the flat lines departing from the sloping one. In order to evaluate the equivalent notch or defect size a_{eq} (6), the parameter $\alpha^2 \cdot a$ can be calculated by using the Stress Intensity Factor (SIF) equality:

$$\alpha^2 a = \frac{1}{\pi}\left(\frac{K_I}{\sigma_g}\right)^2. \tag{11}$$

In the general case of a two-dimensional crack, K_I is the maximum SIF value calculated along the crack front by applying a nominal stress σ_g (Akiniwa et al., 1997). As an example, in case of the surface crack generated by the small drilled holes at

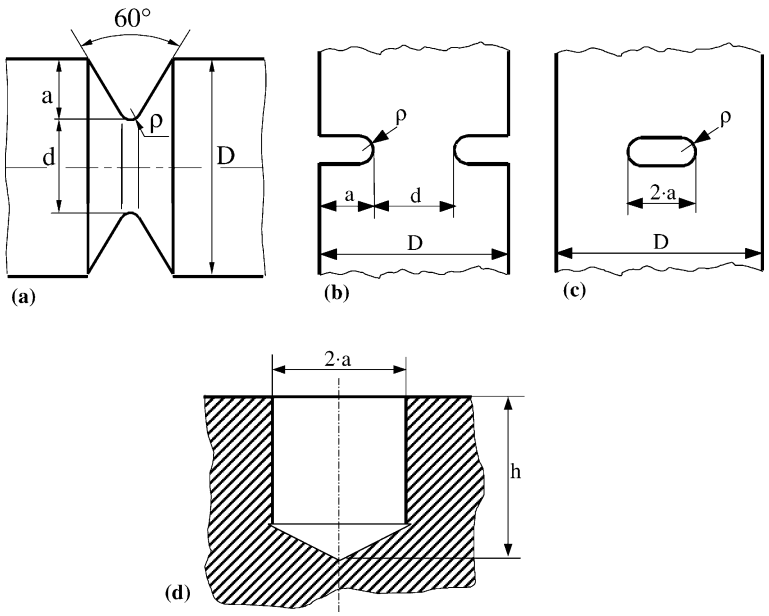

Figure 4. Geometry of specimens weakened by notches and defects: (a) V-shaped notch in a cylindrical bar (CNB), (b) double lateral notch in a flat plate (DENP), (c) hole in a flat plate (CNP), (d) drilled hole in a cylindrical bar (DHB).

the fatigue limit, Murakami and Endo suggested the following equation (Murakami and Endo, 1983):

$$K_I = 0.65\sigma_g\sqrt{\pi\sqrt{\text{area}}}, \tag{12}$$

where "area" is the surface of the defect projected in the direction of the maximum principal stress. In the case of U- and V-notches reported in Table 2, the parameter α was determined by means of accurate finite element analyses where the notch was modelled as a crack having the same depth.

In order to clarify the fatigue behaviour close to the branch line shown in Figure 3, all the available experimental data are plotted in two-dimensional diagrams of Figures 6 and 7 by using the normalised notch size a_{eq}/a^* and the normalised stress concentration factor K_{tg}/K_{tg}*, respectively. Doing so, the branch line obviously collapses into a single point having unit coordinates. Concerning the asymptotic fatigue behaviour of sharp notches shown by the sloping line in Figure 6, substitution of Equation (2) into Equation (7) leads to the expression

$$\frac{K_{tg}}{K_f} = \frac{1}{\sqrt{\frac{\alpha^2 a + a_0}{a^*}}}, \tag{13}$$

where the fatigue reduction factor K_f is defined as the ratio between the plain fatigue limit and the notch fatigue limit, i.e. $K_f = \Delta\sigma_0/\Delta\sigma_{g,th}$. As it is well known such a ratio is equal to one for blunt notches and is increasingly greater than unity the sharper is the notch. Moving to the Frost–Miller diagram shown in Figure 7, the experimental data for blunt notches conform to Equation (8) re-arranged in terms of

Table 2. Geometrical parameters and fatigue limit values of the notched specimens.

Material	Load ratio R	Load type [a]	a (mm)	d (mm)	D (mm)	ρ (mm)	$\zeta = a/\rho$	K_{tg}	$\Delta\sigma_{g,th}$ (MPa)	$\Delta\sigma_0/K_{tg}$ (MPa)	α
0.45	−1	RB	0.005	5	5.01	0.05	0.1	1.68	547	347	1.09
Carbon			0.005	5	5.01	0.02	0.25	2.07	547	281	1.09
Steel			0.005	5	5.01	0.01	0.5	2.54	557	230	1.09
(CNB-Figure 4a)			0.01	5	5.02	0.05	0.2	1.97	484	295	1.09
			0.01	5	5.02	0.02	0.5	2.55	494	228	1.09
			0.01	5	5.02	0.01	1	3.23	484	180	1.09
			0.1	5	5.2	0.6	0.167	1.78	373	328	1.10
			0.1	5	5.2	0.3	0.333	2.13	338	274	1.10
			0.1	5	5.2	0.1	1	3.06	302	190	1.10
			0.1	5	5.2	0.05	2	3.98	320	146	1.10
			0.1	5	5.2	0.02	5	5.86	320	99	1.10
			0.5	5	6	0.6	0.83	3.21	208	181	1.24
			0.5	5	6	0.3	1.67	4.13	174	141	1.24
			0.5	5	6	0.1	5	6.57	162	88.7	1.24
			0.5	5	6	0.05	10	8.97	162	64.9	1.24
			0.5	5	6	0.02	25	13.7	168	42.4	1.24
			0.5	5	6	0.01	50	19.0	168	30.6	1.24
			1.5	5	8	0.6	2.5	7.82	85.4	74.4	1.97
			1.5	5	8	0.3	5	10.3	68.4	56.4	1.97
			1.5	5	8	0.1	15	16.7	61.0	34.8	1.97
			1.5	5	8	0.05	30	23.2	61.0	25.1	1.97
			1.5	5	8	0.02	75	36.0	61.0	16.2	1.97
			1.5	5	8	0.01	150	50.4	63.5	11.6	1.97
0.36	−1	RB	1	13	15	0.2	5	6.45	208	113	1.19
Carbon			0.7	13	14.4	0.2	3.5	5.29	174	137	1.16
Steel			0.5	13	14	0.2	2.5	4.47	162	163	1.14
(CNB-Figure 4a)			0.3	13	13.6	0.2	1.5	3.58	162	203	1.09

Table 2. continued.

Material	Load ratio R	Load type [a]	a (mm)	d (mm)	D (mm)	ρ (mm)	$\zeta = a/\rho$	K_{tg}	$\Delta\sigma_{g,th}$ (MPa)	$\Delta\sigma_0/K_{tg}$ (MPa)	α
			0.15	13	13.3	0.2	0.75	2.74	168	254	1.09
			0.1	13	13.2	0.2	0.5	2.40	168	288	1.09
SAE	−1	AX	0.12	44.21	44.45	0.12	1	3.00	357	202	1
1045			0.25	43.95	44.45	0.25	1	3.00	306	202	1
Steel			0.5	43.45	44.45	0.5	1	3.01	273	201	1
(CNP-Figure 4c)			1.5	41.45	44.45	1.5	1	3.02	231	200	1
			2.5	39.45	44.45	2.5	1	3.04	232	199	1
2024-T351	0	AX	0.12	44.21	44.45	0.12	1	3.00	172	57.4	1
(CNP-Figure 4c)			0.25	43.95	44.45	0.25	1	3.00	113	57.5	1
			0.5	43.45	44.45	0.5	1	3.01	107	57.2	1
			1.5	41.45	44.45	1.5	1	3.02	85.8	56.9	1
	−1	AX	0.12	44.21	44.45	0.12	1	3.00	159	82.8	1
			0.25	43.95	44.45	0.25	1	3.00	123	82.8	1
			0.5	43.45	44.45	0.5	1	3.01	121	82.5	1
			1.5	41.45	44.45	1.5	1	3.02	83.8	82.0	1
G40.11	−1	AX	0.2	69.60	70	0.2	1.00	3.00	336	190	1
Steel			0.48	69.04	70	0.48	1.00	3.00	239	190	1
(CNP-Figure 4c)			4.8	60.40	70	4.8	1.00	3.00	205	190	1
Mild steel	−1	AX	5.08	53.84	64	0.1	50.8	14.9	84.1	28.3	1.12
(0.15% C)			5.08	53.84	64	0.25	20.3	9.75	90.9	43.1	1.12
(DENP-Figure 4b)			5.08	53.84	64	0.5	10.2	7.25	84.1	57.9	1.12
			5.08	53.84	64	1.27	4.00	4.75	104	88.3	1.12
			5.08	53.84	64	7.62	0.67	2.50	156	168	1.12
AISI304 steel											
(CNB-Figure 4a)	−1	AX	5.08	32.84	43	0.05	102	24.0	72.3	30.0	1.308
FeP04 steel	0.1	AX	10	40	60	0.2	50	15.9	52.5	15.5	1.123
(DENP-Figure 4b)						1.25	8	7.17	62.5	34.4	

Table 2. continued.

Material	Load ratio R	Load type [a]	a (mm)	d (mm)	D (mm)	ρ (mm)	$\zeta = a/\rho$	K_{tg}	$\Delta\sigma_{g,th}$ (MPa)	$\Delta\sigma_0/K_{tg}$ (MPa)	α
						2.5	4	5.29	62.7	46.7	
				30		10	1	3.06	96.7	80.7	
					50	0.2	50	16.3	51.7	15.1	1.13
						1.25	8	7.20	57.8	34.3	
						2.5	4	5.38	63.0	45.9	
						10	1	3.07	90.0	80.4	
AA 356-T6	0.1	AX	8	24	40	0.1	80	20.2	29.2	6.93	1.13
Cast Al alloy						1.25	6.4	6.70	35.6	20.9	
(DENP-Figure 4b)						2.5	3.2	4.92	39.9	28.4	

The values of the fatigue limit $\Delta\sigma_{g,th}$ and the theoretical stress concentration factor K_{tg} are all referred to the gross section.
[a] AX = axial load; RB = rotating bending.

Table 3. Geometrical parameters and fatigue limit values of the holed specimens.

Material	Load ratio R	Load type[a]	$2 \cdot a$ (μm)	h (μm)	D (mm)	$\sqrt{\text{area}}$ (μm)	K_{tg}	$\Delta\sigma_{g,th}$ (MPa)	$\Delta\sigma_0/K_{tg}$ (MPa)	$\alpha^2 \cdot a$(μm)
0.13	−1	RB	100	50	10	60	2.00	362	181	25
Carbon			100	100	10	93	2.35	344	146	39
Steel			100	200	10	136	2.50	314	126	58
(DHB-Figure 4d)			200	100	10	119	2.00	314	157	50
			200	200	10	185	2.35	294	125	78
			200	400	10	272	2.50	274	110	115
			500	250	10	298	2.00	284	142	126
			500	500	10	463	2.35	256	109	195
			500	1000	10	681	2.50	236	94.4	288
0.46	−1	RB	40	40	10	37	2.35	470	200	16
Carbon			50	50	10	46	2.35	452	192	20
Steel			50	100	10	68	2.50	452	181	29
(DHB-Figure 4d)			80	40	10	48	2.00	460	230	20
			80	80	10	74	2.35	422	180	31
			80	160	10	109	2.50	402	161	46
			100	50	10	60	2.00	452	226	25
			100	50	10	60	2.00	452	226	25
			100	100	10	93	2.35	402	171	39
			100	100	10	93	2.35	392	167	39
			100	200	10	136	2.50	382	153	58
			200	100	10	119	2.00	402	201	50
			200	200	10	185	2.35	362	154	78
			200	400	10	272	2.50	344	138	115
			500	250	10	298	2.00	362	181	126
			500	500	10	463	2.35	314	134	195
			500	1000	10	681	2.50	294	118	288

The values of the fatigue limit $\Delta\sigma_{g,th}$ and the theoretical stress concentration factor K_{tg} are all referred to the gross section.
[a]RB = rotating bending.

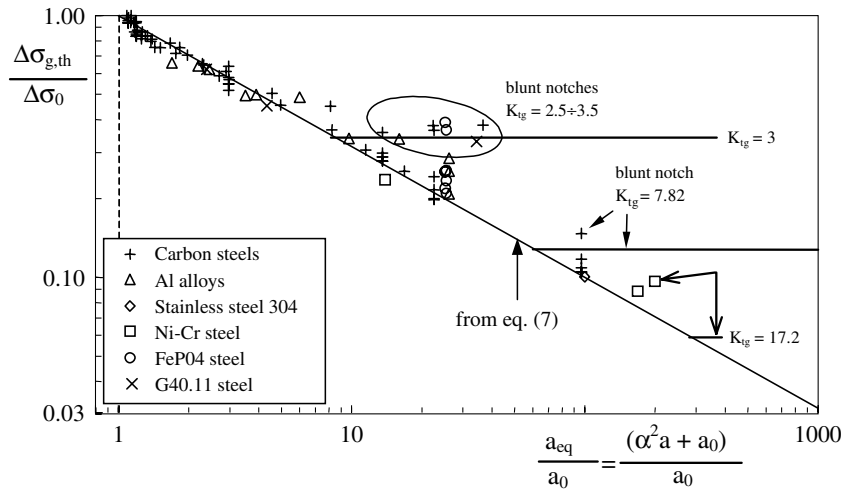

Figure 5. Comparison between Equation (7) and experimental data in terms of equivalent notch depth a_{eq}.

K^*_{tg}/K_f, that is in terms of ratio between the fatigue reduction factor for a crack having the same depth of the notch and the actual fatigue reduction factor. This ratio equals unity for sharp notches and is increasingly greater than unity the more blunt is the notch.

The actual fatigue behaviour is somehow smooth around the knee point. Then, in order to take into account both the defect sensitivity and the notch sensitivity of the material, the following formula is proposed:

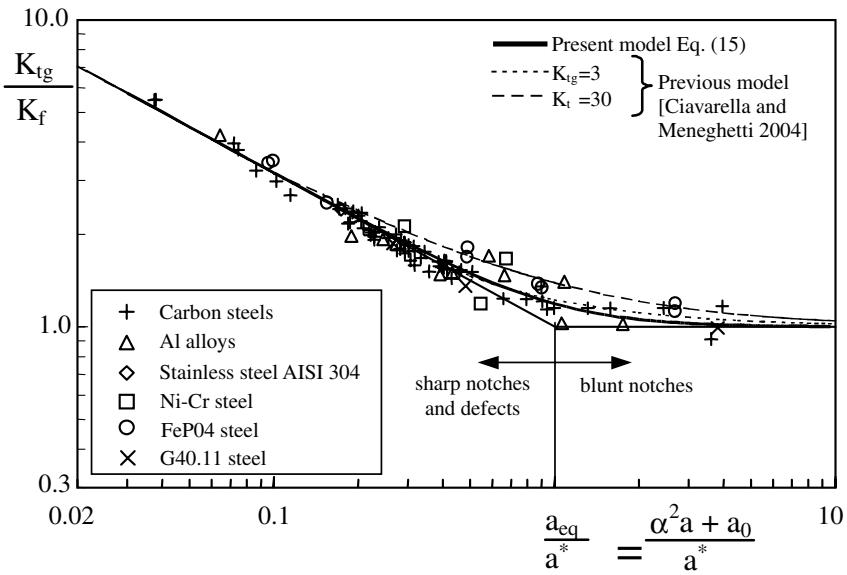

Figure 6. Transition between the sharp and blunt notch fatigue behaviour vs. the equivalent notch size normalised with respect to a^*.

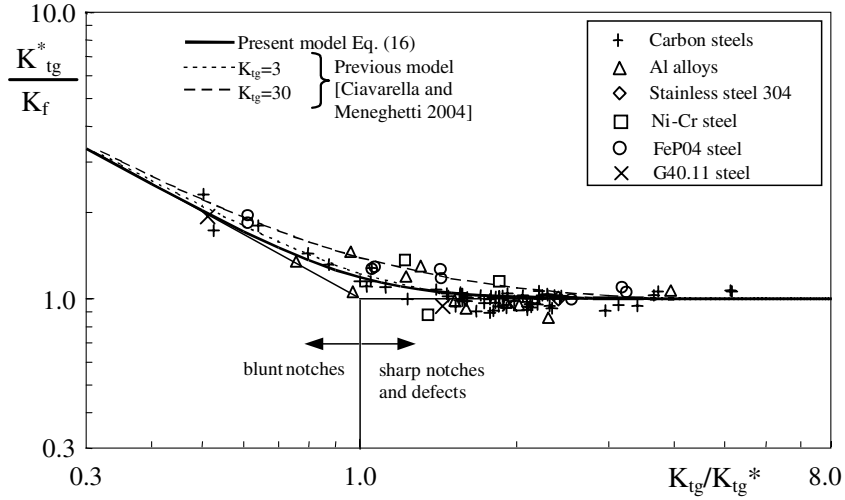

Figure 7. Transition between sharp and blunt notch fatigue behaviour vs. the normalised stress concentration factor.

$$\frac{K_{tg}}{K_f} = \sqrt[4]{1 + \left(\frac{K_{tg}^2 a_0}{\alpha^2 a + a_0}\right)^2}. \tag{14}$$

Equation (14) needs the knowledge of two material properties, ΔK_{th} and $\Delta\sigma_0$, and two stress parameters, K_{tg} and α. By using definitions (2,6), Equation (14) becomes

$$\frac{K_{tg}}{K_f} = \sqrt[4]{1 + \left(\frac{a_{eq}}{a^*}\right)^{-2}}. \tag{15}$$

Alternatively, by taking advantage of Equation (10), Equation (15) can be written in the form:

$$\frac{K_{tg}^*}{K_f} = \sqrt[4]{1 + \left(\frac{K_{tg}^*}{K_{tg}}\right)^4}. \tag{16}$$

Equations (15) and (16) are plotted in Figures 6 and 7, where analytical estimations and experimental data are compared. These Figures display also the results of a very recent model proposed in the literature (Ciavarella and Meneghetti, 2004). Differently from present Equations (15) and (16), that model gave a transition of the fatigue limit curve dependent on K_{tg} value. More precisely, a more smooth transition between blunt and sharp notch fatigue behaviour was expected for higher K_{tg} values. In Figures 6 and 7 two different values of K_{tg} are chosen, namely $K_{tg} = 3$ and $K_{tg} = 30$. The large amount of experimental data show that the transition is substantially independent of K_{tg} and this fact supports the use of Equations (15) and (16). However, one could note that the dependence on K_{tg} was quite weak also in Ciavarella and Meneghetti's model: when the stress concentration factor is varied of one order of magnitude, fatigue strength predictions vary at most of only 17%.

As a final remark, one should note that the two ratios used in the y-axis of Figures 6 and 7 can be also written in the following way:

$$\frac{K_{tg}}{K_f} = \frac{\Delta\sigma_{peak,th}}{\Delta\sigma_0}, \tag{17}$$

$$\frac{K^*_{tg}}{K_f} = \frac{\Delta\sigma_{g,th}}{\Delta\sigma_{g,th,\rho=0}}, \tag{18}$$

where $\Delta\sigma_{peak,th}$ is the fatigue limit in terms of range of the elastic peak stress at the notch tip and, thanks to the definition of K^*_{tg}, $\Delta\sigma_{g,th,\rho=0}$ is the fatigue limit of the cracked geometry, obtained by decreasing the notch root radius to zero and keeping constant the notch depth. This fact gives a sound meaning to diagrams shown in Figures 6 and 7 and provides precise guidelines to notched component design. In fact, thanks to (Equations (15) and (16)), the fatigue limit of a notched components can be expressed with reference to either the fatigue limit of the base material or the fatigue limit of the cracked material, so that material characterisation can be done by using either smooth specimens or, alternatively, cracked specimens.

3. Extension of Kitagawa diagram to open notches

The Kitagawa diagram valid for cracks can be extended to sharp V-notches characterised by a notch opening angle φ greater than zero. The extension proposed here is of a phenomenological type, based on analytical treatment of local models for high cycle fatigue that have recently become available in the literature. Modelling of the actual fatigue phenomenon, consisting in short crack propagation influenced by the notch plastic zone and crack closure effects (Usami, 1987; Verreman and Bailon, 1987; Rose and Wang, 2001) is avoided in the present work.

Consider a V-notch subjected to mode I loading as shown in Figure 8 and the definition of the Notch-Stress Intensity factor according to Gross and Mendelson (1972)

$$K_I^V = \sqrt{2\pi}\lim_{r\to 0}[\sigma_{\theta\theta}(r,\theta=0)r^{1-\lambda_1}], \tag{19}$$

where r and θ are the polar coordinates and λ_1 is the first eingenvalue for Mode I (Williams, 1952).

For V-notched members, we can express the N-SIF as:

$$K_I^V = \alpha_\gamma\sqrt{\pi}a^\gamma\sigma_g = \sqrt{\pi}(\alpha_\gamma^{1/\gamma}a)^\gamma\sigma_g, \tag{20}$$

where

- $\gamma = 1-\lambda_1$ is the degree of singularity of the stress distributions,
- a is a whichever characteristic dimension, for example the notch depth,
- and α_γ is a non-dimensional coefficient, which depends on the component geometry, loading type and notch opening angle φ.

In Equation (20) the quantity between round brackets can be thought as an effective notch depth. Any dimension of a component weakened by a V-notch can be chosen in order to calculate the N-SIF by means of Equation (20). The shape factor α_γ will change accordingly, in order to satisfy the definition of the governing parameter K_I^V given by Equation (19).

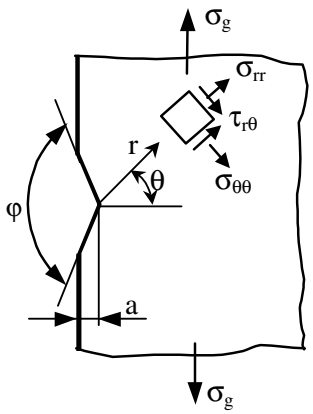

Figure 8. Adopted frame of reference for a sharp V-notch having an opening angle φ and subjected to mode I loading.

3.1. Problem statement

When applied at threshold conditions Equation (20) becomes

$$\Delta\sigma_{g,th} = \frac{\Delta K^{V}_{I,th}}{\sqrt{\pi}\left(\alpha_{\gamma}^{1/\gamma} a\right)^{\gamma}}. \tag{21}$$

In order to account for both "small" and "deep" V-notches, an engineering generalisation of Equation (21) can immediately be written by extending the El-Haddad-Smith-Topper Equation (4). Then

$$\Delta\sigma_{g,th} = \frac{\Delta K^{V}_{I,th}}{\sqrt{\pi}\left(\alpha_{\gamma}^{1/\gamma} \cdot a + a_0^{V}\right)^{\gamma}}, \tag{22}$$

where the parameter a_0^{V}, to be found later, accounts for the sensitivity to "small" V-notches and can be thought of as the natural extension of the material parameter a_0 (El-Haddad et al., 1979).

In order to apply Equation (21) the threshold value of the N-SIF, $\Delta K^{V}_{I,th}$ should be experimentally evaluated. This was done, for example, for fillet-welded joints (Lazzarin and Tovo, 1998; Atzori and Meneghetti, 2001; Lazzarin and Livieri, 2001), where fatigue crack initiation occurred at the weld toe and the local toe geometry was assumed to be a sharp V-notch with a notch angle equal to 135°. On the other hand, standard fracture mechanics tests provide the threshold range of the SIF for a crack, i.e. the value of ΔK_{th}. Then Equation (21) can be applied as soon as a link between $\Delta K_{1,th}$ and ΔK_{th} is established: this task can be accomplished on the basis of known local models for fatigue limit estimations. Finally the characteristic value a_0^{V} of the effective notch depth can be found by forcing into Equation (21) the condition $\Delta\sigma_{g,th} = \Delta\sigma_0$ when $a = a_0^{V}$. By so doing, one obtains

$$a_0^{V} = \left(\frac{\Delta K^{V}_{I,th}}{\sqrt{\pi}\Delta\sigma_0}\right)^{1/\gamma}. \tag{23}$$

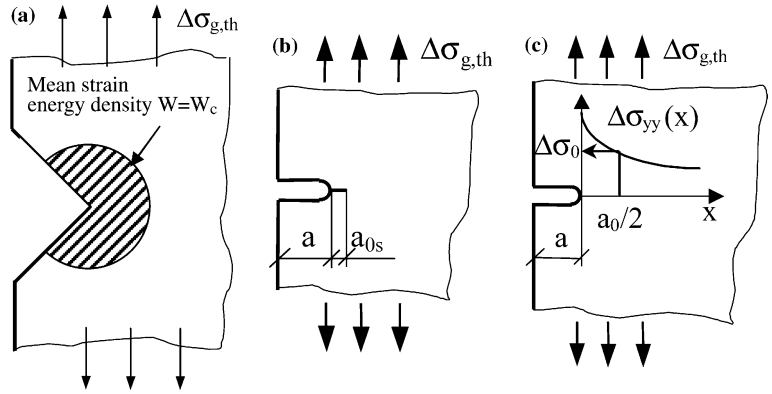

Figure 9. Three different models for fatigue limit assessments. Models are based on Finite-Volume Energy (a), Fracture Mechanics (b) and the Point Method (c).

In the next paragraphs three local approaches available in the literature will be used to derive a relation between ΔK_{th} and $\Delta K_{1,th}$ and an expression for a_0^V: the local strain energy approach, the Fracture Mechanics approach and the Point Method.

3.2. Application of the local approach based on the strain energy in a finite size volume

The mean value of the strain energy within a finite size volume located at the notch tip was proposed as a parameter suitable for summarising static strength data from V-notched specimens in brittle material as well as high cycle fatigue properties of mechanical components weakened by the same geometrical features (Lazzarin and Zambardi, 2001; Lazzarin et al., 2003, 2004). The model is presented in Figure 9a: the critical volume surrounding the notch tip was assumed to be a circular sector of radius R. The size of the structural volume and the critical energy were thought of as a material parameters at the fatigue limit, for a given nominal load ratio. The energy within the structural volume was derived by using linear elastic stress distributions ahead of the notch tip. Then the critical energy at the fatigue limit and the radius of the structural volume were found by matching the experimental conditions for a plain and a cracked specimen, respectively. By so doing, the authors were able to deliver Equation (24), which enables one to estimate the threshold range of the N-SIF from the plain fatigue limit and the threshold SIF for long cracks:

$$\Delta K_{I,th}^V = \beta_{\overline{w}} \Delta\sigma_0 \left(\frac{\Delta K_{th}}{\Delta\sigma_0} \right)^{2\cdot\gamma} = \beta_{\overline{w}} \Delta\sigma_0^{(1-2\gamma)} \Delta K_{th}^{2\gamma}. \tag{24}$$

Values for β_w are given in Table 4 with reference to plain strain conditions and a Poisson's coefficient $\nu = 0.3$. Substitution of Equation (24) into Equation (23) leads to

$$a_0^V = \left[\beta_{\overline{w}}^{1/\gamma} \pi^{\left(1-\frac{1}{2\gamma}\right)} \right] a_0 = \alpha_{0\gamma,\overline{w}} a_0. \tag{25}$$

Table 4. Values of parameters β and $\alpha_{0\gamma}$.

φ(deg)	$\gamma = 1-\lambda_1$	Local energy		Fracture mechanics		Point method	
		β_{w}	$\alpha_{0\gamma,\overline{\mathrm{w}}}$	β_{LEFM}	$\alpha_{0\gamma,\mathrm{LEFM}}$	β_{PM}	$\alpha_{0\gamma,\mathrm{PM}}$
0	0.5	1	1	1	1	1	1
15	0.4998	0.9805	0.9609	1	0.999	1	1
30	0.4986	0.9653	0.9287	1.002	1.001	1.003	1.002
45	0.495	0.9578	0.9061	1.011	1.011	1.009	1.007
60	0.4878	0.9610	0.8956	1.030	1.032	1.023	1.017
90	0.4555	1.017	0.9274	1.107	1.118	1.085	1.070
120	0.3843	1.186	1.103	1.277	1.338	1.237	1.232
135	0.3264	1.345	1.350	1.424	1.605	1.376	1.446
150	0.248	1.591	2.032	1.641	2.303	1.589	2.022
160	0.1813	1.828	3.719	1.846	3.934	1.796	3.382
170	0.1	2.152	21.846	2.125	19.255	2.086	16.00

Values of $\alpha_{0\gamma,\overline{\mathrm{w}}}$ are also listed in Table 4 for different notch angles. It is worth noting that, unlike the shape factor α_γ of Equation (20), the factor $\alpha_{0\gamma,\overline{\mathrm{w}}}$ depends only on the notch opening angle and not on the component geometry.

Substitution of Equation (25) into Equation (22) leads to the following El-Haddad type equation for sharp V-notches:

$$\Delta\sigma_{\mathrm{g,th}} = \frac{\Delta K^{\mathrm{V}}_{\mathrm{I,th}}}{\sqrt{\pi}\left(\alpha_\gamma^{1/\gamma} a + \alpha_{0\gamma,\overline{\mathrm{w}}}\, a_0\right)^{\gamma}}. \tag{26}$$

Accuracy of Equation (26) will be later proved against a number of experimental results from fatigue tests.

3.3. Application of the local approach based on fracture mechanics

It is well known that the fatigue limit of sharp notches is the threshold condition for the propagation of small cracks nucleated at the notch tip (Lukas and Klesnil, 1978; Smith and Miller, 1978; Tanaka and Nakai, 1983). The authors of the present paper found the small crack size to be equal to $a_{0\mathrm{s}}$, being $a_{0\mathrm{s}} = a_0/1.12^2$ (Atzori et al., 2002a), as depicted in Figure 9b.

The SIF of a small crack ($a_{0\mathrm{s}}$ in length) at the tip of a notch can be calculated by means of Albrecht–Yamada's simplified approach which makes use of Bueckner's superposition principle (Bueckner, 1970; Albrecht and Yamada, 1977)

$$K_{\mathrm{I}} = 1.12\frac{2}{\pi}\int_0^{a_{0\mathrm{s}}} \frac{\sigma_{\theta\theta}(r,0)}{\sqrt{a_{0\mathrm{s}}^2 - r^2}}\mathrm{d}r \cdot \sqrt{\pi a_{0\mathrm{s}}}. \tag{27}$$

The asymptotic stress field is given by

$$\sigma_\theta(r,0)=\frac{K_{\mathrm{I}}^{\mathrm{V}}}{\sqrt{2\pi}r^{\gamma}}. \tag{28}$$

Substitution of this expression into Equation (27), taking into account the definition of $a_{0\mathrm{s}}$ and changing the variable inside the integral leads to

$$K_{\mathrm{I}}^{\mathrm{V}}=\left[1.12^{(2\gamma-1)}\cdot\frac{\sqrt{2}}{\pi}\cdot\int_0^1\frac{1}{\xi^{\gamma}\cdot\sqrt{1-\xi^2}}\mathrm{d}\xi\right]^{-1}K_{\mathrm{I}}a_0^{(\gamma-(1/2))}. \tag{29}$$

At the threshold condition, Equation (29) gives

$$\Delta K_{\mathrm{I,th}}^{\mathrm{V}}=\left[1.12^{(2\gamma-1)}\sqrt{2}\pi^{(\gamma-(3/2))}\int_0^1\frac{1}{\xi^{\gamma}\cdot\sqrt{1-\xi^2}}\mathrm{d}\xi\right]^{-1}\Delta\sigma_0^{(1-2\gamma)}\Delta K_{\mathrm{th}}^{2\gamma} \tag{30}$$

or, more simply

$$\Delta K_{\mathrm{I,th}}^{\mathrm{V}}=\beta_{\mathrm{LEFM}}\Delta\sigma_0^{(1-2\gamma)}\Delta K_{\mathrm{th}}^{2\gamma}. \tag{31}$$

Equation (31) can be directly compared with Equation (24): the threshold value of the N-SIF can be obtained from the threshold SIF for long cracks and the material fatigue limit. In both equations β depends only on the notch opening angle.

Substitution of Equation (31) into Equation (23) leads to an equation formally analogous to Equation (25), provided that β_{w} must be substituted by β_{LEFM} in order to obtain the expression for $\alpha_{0\gamma,\mathrm{LEFM}}$.

Albrecht–Yamada's simplified approach results in increasing errors as the notch opening angle decreases. As an alternative, for estimating the SIF value for a crack originated from a sharp V-notch in (Figure 9a), the following formula can be used, which was derived from one proposed by Murakami (1990) and is valid for a semi-infinite plate subjected to mode-I tension loading

$$K_{\mathrm{I}}=C(\varphi)\,K_I^{V}\sqrt{\pi}b^{((1/2)-\gamma)}, \tag{32}$$

where b is the length of the crack emanated from the V-notch and $C(\varphi)$ is the following function

$$C(\varphi)=-4.658\times10^{6}\cdot\varphi^2+1.840\times10^{4}\cdot\varphi+5.629\times10^{-1} \tag{33}$$

φ being in degrees.

By indicating with "a" the V-notch depth, estimations for K_{I} based on Equation (32) with an error lower than 5% result in some limits of applicability. Such limits are: when $0^\circ\le\varphi\le90^\circ$ then the ratio b/a must be lower than 0.1, when $90^\circ<\varphi\le120^\circ$ then the ratio b/a must be lower than 0.2 and, finally, when $120^\circ\le\varphi\le160^\circ$ then the ratio b/a must be lower than 0.5.

By imposing $b=a_{0\mathrm{s}}$ in Equation (32) at threshold conditions we have

$$\Delta K_{\mathrm{th}}=C(\varphi)\cdot\Delta K_{\mathrm{I,th}}^{\mathrm{V}}\cdot\sqrt{\pi}\cdot a_{0\mathrm{s}}{}^{(\frac{1}{2}-\gamma)}. \tag{34}$$

Substitution of definition of a_{0s} into Equation (34) leads again to an expression of the type

$$\Delta K_{I,th}^{V} = \beta_{LEFM} \cdot \Delta\sigma_0^{1-2\cdot\gamma} \cdot \Delta K_{th}^{2\cdot\gamma}, \tag{35}$$

where the parameter β must be updated according to the present model

$$\beta_{LEFM} = \frac{1.12^{1-2\cdot\gamma}}{C(\varphi)\cdot\pi^{\gamma}} \tag{36}$$

Values of β_{LEFM} and $\alpha_{0\gamma,LEFM}$, the latter obtained by simply updating Equation (25), are given in Table 4. This table makes it possible a comparison with the coefficients already determined on the basis of the energy-based model.

3.4. Application of the point method

Sound basis to all critical distance approaches are in pioneering paper by Ritchie et al. (1973). More recently, the parameter a_0 was explicitly included in the critical distance methods when applied to fatigue limit assessments of components weakened by cracks, crack-like notches (Tanaka, 1983; Lazzarin et al., 1997)) and common notches (Taylor, 1999). For a given notch subjected to mode I loading, the "Point method" results in a distance from the notch tip equal to $a_0/2$ (Figure 9c) to obtain the fatigue limit of plain specimens.

By imposing the condition invoked by the point method into Equation (28), at threshold one obtains

$$\frac{\Delta K_{I,th}^{V}}{\sqrt{2\pi}\left(\frac{a_0}{2}\right)^{\gamma}} = \Delta\sigma_0. \tag{37}$$

Recalling the definition of a_0, Equation (37) becomes

$$\Delta K_{I,th}^{V} = \frac{\sqrt{2}}{2^{\gamma}}\pi^{((1/2)-\gamma)}\Delta\sigma_0^{(1-2\gamma)}\Delta K_{th}^{2\gamma} = \beta_{PM}\Delta\sigma_0^{(1-2\gamma)}\Delta K_{th}^{2\gamma}, \tag{38}$$

which is again formally identical to Equation (24), where now parameter β_{PM}, according to the point method, is given by

$$\beta_{PM} = \frac{\sqrt{2}}{2^{\gamma}}\pi^{((1/2)-\gamma)}. \tag{39}$$

Thus the expression for $\alpha_{0\gamma,PM}$ as a function of β_{PM} is analogous to Equation (25). Values of β_{PM} and $\alpha_{0\gamma,PM}$ are also reported in Table 4.

3.5. Comparison among the considered approaches

Fatigue limit of a sharp V-notch in terms of nominal stresses can be carried out by using Equations (22) and (23), where $\Delta K_{I,th}^{V}$ is linked to two material parameters, namely the plain fatigue limit $\Delta\sigma_0$ and the threshold value of the stress intensity factor range for long cracks ΔK_{th}.

Since the three models considered here leads to expressions for $\Delta K_{I,th}^{V}$ and a_0^{V} which are formally identical to one another, a comparison can be made in terms of

the parameters β, as shown in Table 4. The parameter β equals unity when the notch opening angle is zero (the crack case) and it is is nearly constant up to a V-notch opening angle of about 100°. For greater values of the angle, β rapidly increases beyond unity.

As far as $\alpha_{0\gamma}$ is concern, the three criteria conform to an expression formally equal to Equation (25). From Table 4 it can be deduced that the cut-off value of the effective notch depth a_0^V (obeying Equation (25)) can be considered nearly equal to a_0 when the notch angle is less than 100°. Beyond such a value, a_0^V rapidly increases. As an example, for a notch opening angle equal to 160°, a_0^V ranges from $3.4a_0$ to $3.7a_0$.

Finally, Figure 10 shows the generalised Kitagawa diagram for sharp V-notches plotted according to Equation (22). The effect of the notch opening angle on the cut-off value a_0^V can be appreciated. The only geometrical feature that distinguishes the theoretical curves plotted in Figure 10 is the notch opening angle φ, which determines the degree of singularity of the local stress distributions (Williams, 1952). Independence on the chosen dimension "a", which accounts for the scale effect, is assured by the adoption of the effective dimension $(\alpha_\gamma^{1/\gamma} \cdot a)$ in the abscissa of the diagram: for a given notch opening angle, the fatigue limit is a unique function of $(\alpha_\gamma^{1/\gamma} \cdot a)$, as shown by Equation (20), $\Delta K_{I,th}^V$ being a material parameter.

4. Experimental validation of the generalised Kitagawa diagram

The accuracy of Equation (22) was tested against the experimental data obtained by Kihara and Yoshi by testing mild and high strength steel plates (Kihara and Yoshii, 1991). Specimen geometry is shown in Figure 11: three series of specimens were characterised by lateral V-notches with notch angles equal to 90° and 120°. Other two series were weld-like geometries, having an opening angle equal to 135° and 150°. Mode II stress distributions are absent in the former three series, while they are

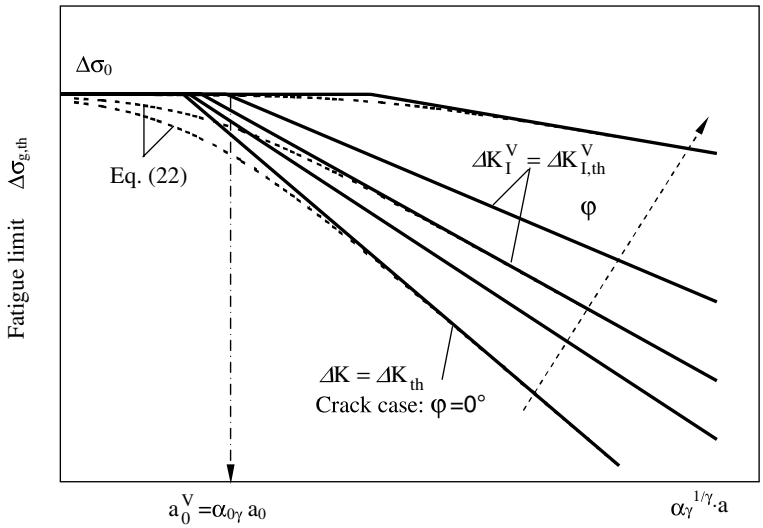

Figure 10. Generalised Kitagawa diagram for V-notches.

negligible in the latter two series, due to the great value of the notch opening angle. During the fatigue tests, the adopted load ratio was equal to 0.05, while tests were stopped when the crack length was about 0.2 mm.

A comparison between numerical predictions and experimental results is reported in Figures 12 and 13 for the two materials. Theoretical calculations were performed by means of the energy-based model, i.e. by means of Equation (26) combined with Equation (24). Values of the shape coefficient α_γ used in Equation (26) were calculated by means of accurate finite element analyses and are reported in Figure 11.

The dimension "a" reported in the abscissa is the depth of the V-notch for the plates containing lateral V-notches while is the main plate thickness for the weld-like geometries. Had the dimension "a" been chosen equal to the specimen width for all cases, then diagrams reported in Figures 12 and 13 would have been unchanged by virtue of Equation (20). That is because the cut-off dimension a_0^V defined by Equation (23) does depends only on the notch opening angle (see Equation (27)).

Both figures show the good agreement between the theoretical models and the experimental results. Due to the small variability of coefficients (see Table 4 for a notch angle ranging from 90° to 150°) the comparison between theoretical predictions and experimental results would not have changed by using the other two models.

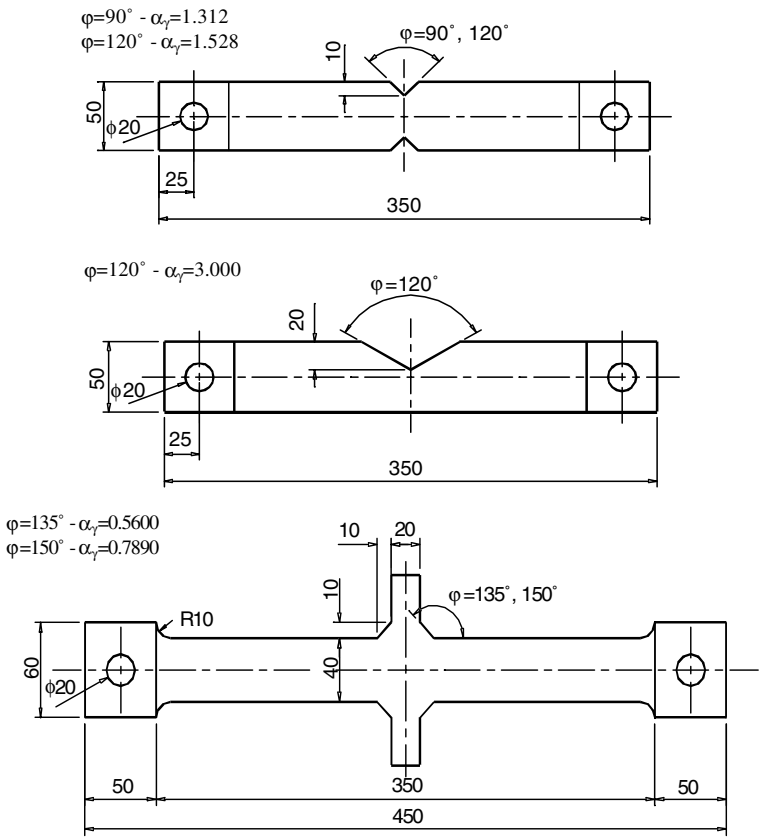

Figure 11. Geometry of the specimens used by Kihara and Yoshii (Kihara and Yoshii, 1991). All dimensions in mm.

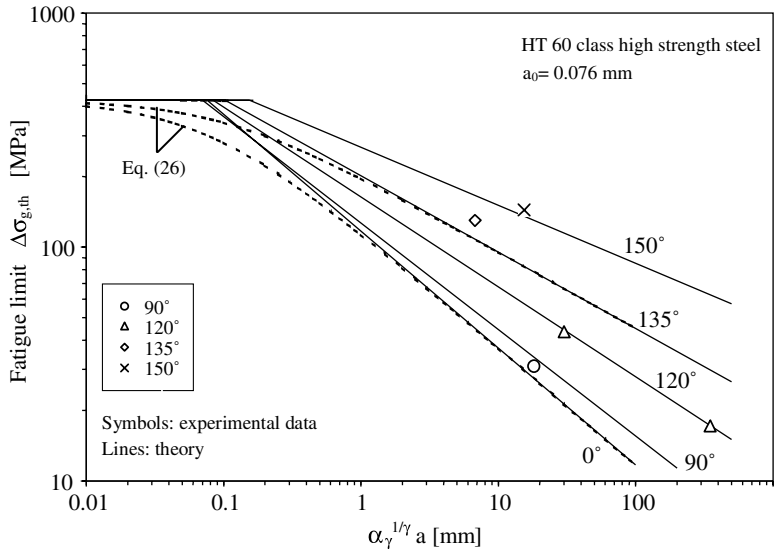

Figure 12. Comparison between Equation (26) and experimental results for the HT60 high strength steel.

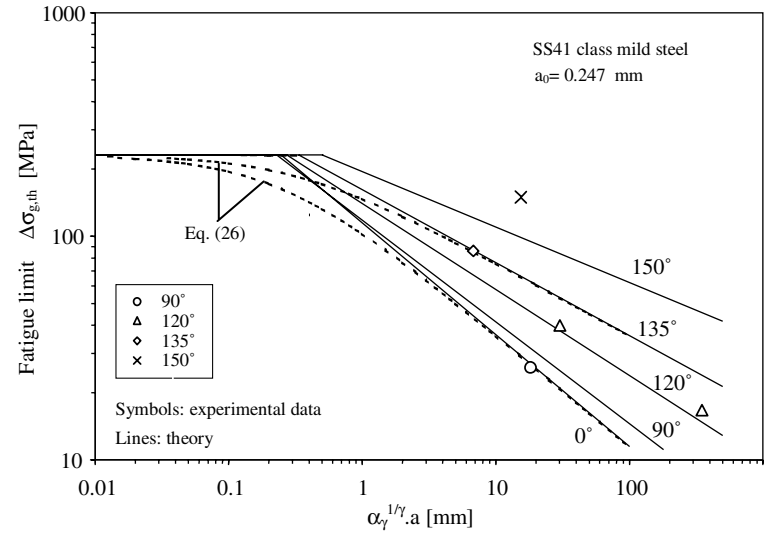

Figure 13. Comparison between Equation (26) and experimental results for the SS41 mild steel.

5. Final remarks

In order to find the real dimension "a" in correspondence to a_0^{V}, i.e. the reference dimension of the component below which the fatigue behaviour is not affected by the presence of the notch, the following formula should be applied:

$$a_{\mathrm{D}\gamma} = \frac{\alpha_{0\gamma} \cdot a_0}{\alpha_\gamma^{1/\gamma}}, \tag{40}$$

$\alpha_{0\gamma}$ being evaluated according to one of the models presented in the present work. For example, in the case of the weld-like specimens with $\varphi = 135^\circ$ made of SS41 steel

(see Figure 11), the cut-off thickness $a_{D\gamma}$ is equal to $1.97\,\text{mm} \approx 2\,\text{mm}$ ($\alpha_{0\gamma} = 1.350$, $\alpha_\gamma = 0.560$, $\gamma = 0.326$, $a_0 = 0.247\,\text{mm}$). It is worth noting that in the case of a crack $\alpha_{0\gamma}$ equals unity and $\gamma = 0.5$ so that Equation (40) simply matches the expression $a_D = a_0/\alpha^2$ (Atzori et al., 2003)

Finally an extension of Equation (14) is proposed in order to include V-notches with large opening angles. By updating the exponents the following equation is obtained:

$$\frac{K_{tg}}{K_f} = \left[1 + \left(\frac{K_{tg}^{1/\gamma} \cdot \alpha_{0\gamma} \cdot a_0}{\alpha_\gamma^{1/\gamma} \cdot a + \alpha_{0\gamma} \cdot a_0} \right)^{1/\gamma} \right]^{\gamma^2}. \tag{41}$$

The proposed equation can be used in order to estimate the fatigue reduction factor K_f for members weakened by V-notches of arbitrary opening angle and notch root radius subjected to prevailing mode I stress distribution. Figure 14 plots Equation (41) for different notch opening angles. It can be thought of as an extension to V-notches of the diagram already shown in Figure 6 for U-notches. Symbols in the abscissa of Figure 14 have been conveniently updated, being now

$$a_{eq,\gamma} = \alpha_\gamma^{1/\gamma} a + \alpha_{0\gamma} a_0 \tag{42}$$

and

$$a_\gamma^* = K_{tg}^{1/\gamma} \alpha_{0\gamma} a_0. \tag{43}$$

Figure 14 highlights that scale effect in fatigue of sharp V-notches is almost the same when the notch opening angle ranges from 0° to 90°, being the singularity exponent in Williams equation almost constant (Williams, 1952). This fact provides a justification to what has been done in the first part of the present work, where V-notches having a notch opening angle equal to 60° have been treated as U-notches.

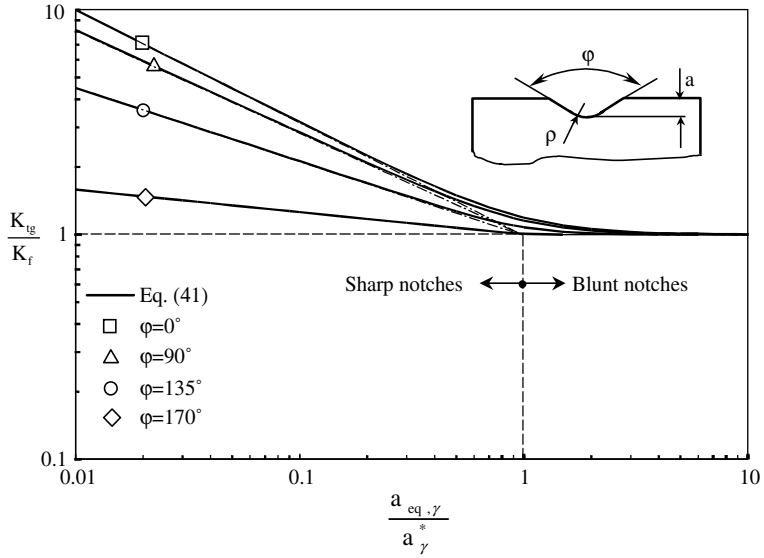

Figure 14. Scale effect of V-notched members subjected to mode I stress distribution in high cycle fatigue conditions.

6. Conclusions

The present work has presented a unified treatment of U- and V-notches having an arbitrary notch opening angle and notch tip radius and subjected to prevailing mode I fatigue loadings. In particular the problem of estimating the fatigue limit in terms of applied nominal stresses has been addressed and formulas for estimating the ratio between the elastic stress concentration factor and the fatigue reduction factor have been proposed.

Concerning U-notched members, Equation (14) is proposed which satisfy the two asymptotic fatigue behaviours of smooth and cracked components. An engineering approximation is assumed in the fatigue regimes where the material exhibits a sensitivity to defects and to notches, respectively, the former being the same proposed by El-Haddad-Smith-Topper. Two material parameters are needed among the following three ones: the plain fatigue limit, the threshold value of the SIF for long cracks and the El-Haddad-Smith-Topper length parameter. The new formula was validated by means of about 90 experimental fatigue limits generated by 12 different materials, including carbon steels, low strength steels, high strength steels, wrought aluminium alloys and one cast aluminium alloy.

Concerning V-notched members, an analytical relation was established between the threshold value of the N-SIF and the threshold SIF for long cracks. This task could be accomplished by applying local approaches valid in notch fatigue that became recently available from literature. By so doing, additional material parameters were not needed in order to extend the Kitagawa diagram, valid for cracks, to sharp V-notches. The new diagram was validated by means of experimental results taken from literature generated by low and high strength steels. As a results Equation (22) is proposed, which account also for the short notch effect by extending the El-Haddad et al. equation proposed in the past.

Finally Equation (41) is proposed for fatigue limit estimation of V-notched members, which encompasses all cases of practical interest, i.e. short/long notches with arbitrary notch opening angles and notch tip radii. Lack of experimental data did not enabled us to validate the proposed formula for open V-notches in the region where notch sensitivity or defect sensitivity exist. In any case, the asymptotic fatigue behaviours, namely the plain fatigue limit, the full scale effect and the full notch sensitivity, are correctly matched.

Acknowledgements

The authors wish to thank the Italian Ministry of University and Scientific Research and the University of Padova for funding this research (project codes: PRIN 2004082252-005 and CPDA-035135).

References

Albrecht, P. and Yamada, K. (1977). Rapid calculation of stress intensity factors. *Journal of the Structural Division*, ASCE **103**, 377–389.

Akiniwa, Y., Zhang, L.M. and Tanaka, K. (1997). Prediction of the fatigue limit of cracked specimens based on the cyclic R-curve method. *Fatigue and Fracture of Engineering Materials and Structures* **20**, 1387–1398.

Atzori, B. and Lazzarin, P. (2001). Notch sensitivity and defect sensitivity under fatigue loading: two sides of the same medal. *International Journal of Fracture* **107**, L3–L8.

Atzori, B. and Meneghetti, G. (2001). Fatigue strength of fillet welded structural steels: finite elements, strain gauges and reality. *International Journal of Fatigue* **23**(8), 713–721.

Atzori, B. and Lazzarin, P. (2002). A three dimensional graphical aid to analyze fatigue crack nucleation and propagation phases under fatigue limit conditions. *International Journal of Fracture* **118**, 271–284.

Atzori, B., Lazzarin, P., Meneghetti, G. (2002a). Interpretation of fatigue limit of materials based on micromechanics. In: *Proceedings of the 8th International Fatigue Congress*. Edited by Bloom, A. F. EMAS, 1873–1880.

Atzori, B., Lazzarin, P. and Meneghetti G. (2002b). Sensitivity to defects and fracture mechanics for metallic materials under fatigue loading. In: *Proceedings of the 14th European Conference on Fracture*. Edited by Neimitz, A., Rokach, I.V., Kocanda, D., Golos, K. EMAS, 129–136.

Atzori, B., Lazzarin, P. and Meneghetti, G. (2003). Fracture mechanics and notch sensitivity. *Fatigue and Fracture of Engineering Materials and Structures* **26**, 257–267.

Atzori, B., Meneghetti, G. and Susmel, L. (2004). Fatigue behaviour of AA356-T6 cast aluminium alloy weakened by cracks and notches. *Engineering Fracture Mechanics* **71**, 759–768.

Bueckner, H.F. (1970). A novel principle for the computation of stress intensity factors. *Zeitschrift für angewandte Mathematik und Mechanik* **50**, 529–546.

Ciavarella, M. and Meneghetti, G. (2004). On fatigue limit in the presence of notches: classical vs. recent unified formulations. *International Journal of Fatigue* **26**, 289–298.

Du Quesnay, D.L., Yu, M.T. and Topper, T.H. (1988). An analysis of notch size effect on the fatigue limit. *Journal of Testing and Evaluation* **4**, 375–385.

El Haddad, M.H., Topper, T.H. and Smith, K.N. (1979). Prediction of non-propagating cracks. *Engineering Fracture Mechanics* **11**, 573–584.

Frost, N.E. (1957). Non-propagating cracks in Vee-notched specimens subjected to fatigue loading. *Aeronautical Quarterly*. VIII, 1–20.

Frost, N.E. (1959). A relation between the critical alternating propagation stress and crack length for mild steel. *Proceedings of the Institution of Mechanical Engineers* **173**, 811–834.

Frost, N.E. (1961). A note on the behaviour of fatigue cracks. *Journal of the Mechanics and Physics of Solids* **3**, 143–151.

Frost, N.E., Marsh, K.J., Pook, L.P. (1974). Metal Fatigue. Oxford University Press, Oxford.

Gross, B. and Mendelson, A. (1972). Plane elastostatic analysis of V-notched plates. *International Journal of Fracture Mechanics* **8**, 267–276.

Harkegard, G. (1981). An effective stress intensity factor and the determination of the notched fatigue limit. In: *Fatigue Thresholds: Fundamentals and Engineering Applications* Edited by Backlund, J., Blom, A.F., Beevers, C.J. Vol. 2, Chameleon Press Ltd., London, 867–879.

Kihara, S. and Yoshii, A. (1991). A strength evaluation method of a sharply notched structure by a new parameter, 'the equivalent stress intensity factor'. *JSME International Journal* **34**, 70–75.

Kitagawa, H. and Takahashi, S. (1976). Applicability of fracture mechanics to very small cracks in the early stage. *Proceedings of the 2nd International Conference on Mechanical Behaviour of Materials*, pp. 627–631.

Lazzarin, P., Tovo, R. and Meneghetti, G. (1997). Fatigue crack initiation and propagation phases near notches in metals with low notch sensitivity. *International Journal of Fatigue* **19**, 647–657.

Lazzarin, P. and Tovo, R. (1998). A notch intensity factor approach to the stress analysis of welds. *Fatigue and Fracture of Engineering Materials and Structures* **21**, 1089–1103.

Lazzarin, P. and Livieri, P. (2001). Notch stress intensity factors and fatigue strength of aluminium and steel welded joints. *International Journal of Fatigue* **23**, 225–232.

Lazzarin, P. and Zambardi, R. (2001). A finite-volume-energy based approach to predict the static and fatigue behaviour of components with sharp V-shaped notches. *International Journal of Fracture* **112**, 275–298.

Lazzarin, P., Lassen T. and Livieri, P. (2003). A Notch Stress Intensity approach applied to fatigue life predictions of welded joints with different local toe geometry. *Fatigue and Fracture of Engineering Materials and Structures* **26**, 49–48.

Lazzarin, P., Sonsino CM. and Zambardi R. (2004). A Notch Stress Intensity approach to predict the fatigue behaviour of T butt welds between tube and flange when subjected to in–phase bending and torsion loading. *Fatigue and Fracture of Engineering Materials and Structures* **27**, 127–141.

Lukas, P. and Klesnil, M. (1978). Fatigue limit of notched bodies. *Material Science and Engineering* **34**, 61–66.

Lukas, P., Kunz, L., Weiss, B. and Stickler, R. (1986). Non-damaging notches in fatigue. *Fatigue and Fracture of Engineering Materials and Structures* **9**, 195–204.

McEvily, A.J., Endo, M. and Murakami, Y. (2003). On $\sqrt{area}$ relationship and the short fatigue crack threshold. *Fatigue and Fracture of Engineering Materials and Structures* **26**, 269–278.

Murakami, Y. (1990). Stress Intensity Factor Handbook. (Edited by Y. Murakami), Pergamon Press, New york.

Murakami, Y. and Endo, M. (1983). Quantitative evaluation of fatigue strength of metals containing various small defects or cracks. *Engineering Fracture Mechanics* **17**, 1–15.

Murakami, Y. and Endo, M. (1994). Effects of defects, inclusions and inhomogeneities on fatigue strength. *International Journal of Fatigue* **16**, 163–182.

Nisitani, H. and Endo, M. (1988). Unified treatment of deep and shallow notches in rotating bending fatigue. ASTM STP924, *Basic Questions in Fatigue* **1**, 136–153.

Ritchie, R.O., Knott, J.F. and Rice, J.R. (1973). On the relation between critical tensile stress in fracture toughness in mild steel. *Journal of the Mechanics and Physics of Solids* **21**, 395–410

Rose, L.R.F. and Wang, C.H. (2001). Self-similar analysis of plasticity-induced closure of small fatigue cracks. *Journal of the Mechanics and Physics of Solids* **49**, 401–429.

Smith, R.A. and Miller, K.J. (1978). Prediction of fatigue regimes in notched components. *International Journal of Mechanical Sciences* **20**, 201–206.

Tanaka, K. (1983). Engineering formulae for fatigue strength reduction due to crack-like notches. *International Journal of Fracture* **22**, R39–R45.

Tanaka, K. and Nakai, Y. (1983). Propagation and non propagation of short fatigue cracks at a sharp notch. *Fatigue and Fracture of Engineering Materials and Structures* **6**, 315–327.

Tanaka, K. and Akiniwa, Y. (1987). Notch geometry effect on propagation threshold of short fatigue cracks in notched components. In: *Proceedings of the 3rd International Conference on Fatigue and Fatigue Thresholds "Fatigue '87"*, Edited by Ritchie, R.O., Starke Jr, E.A. 739–748.

Taylor, D. (1999). Geometrical effects in fatigue: a unifying theoretical model. *International Journal of Fatigue* **21**, 413–420.

Ting, J.C. and Lawrence, F.V. (1993). A crack closure model for predicting the threshold stresses of notches. *Fatigue and Fracture of Engineering Materials and Structures***16**, 93–114.

Usami, S. (1987). Short crack fatigue properties and component life estimation. In: *Current Research on Fatigue Cracks*. Edited by Tanaka, T., Jono, M., Komai K. Elsevier, pp. 119–147.

Verreman, Y. and Bailon, J. (1987). Fatigue of V-notched members: short crack behaviour and endurance limit. *Engineering Fracture Mechanics* **28**, 773–783.

Williams, M.L. (1952). Stress singularities resulting from various boundary conditions in angular corners of plates in extension. *Journal of Applied Mechanics* **19**, 526–528.